

**Technoeconomic analysis of corn stover conversion by decentralized pyrolysis and electrocatalysis**

Journal:	<i>Sustainable Energy & Fuels</i>
Manuscript ID	SE-ART-11-2021-001881.R1
Article Type:	Paper
Date Submitted by the Author:	29-Mar-2022
Complete List of Authors:	Das, Sabyasachi; Michigan State University Anderson, James; Ford Motor Company, Research & Advanced Engineering De Kleine, Robert; Ford Motor Company, Research and Advanced Engineering Wallington, Timothy; Ford Motor Company, Research & Advanced Engineering Jackson, James; Michigan State University, Chemistry Saffron, Christopher; Michigan State University, Biosystems and Agricultural Engineering, Chemical Engineering and Material Science

Technoeconomic analysis of corn stover conversion by decentralized pyrolysis and electrocatalysis

Sabyasachi Das^a, James E. Anderson^b, Robert De Kleine^b, Timothy J. Wallington^b, James E. Jackson^c, Christopher M. Saffron^{a,d*}

^a*Department of Chemical Engineering and Materials Science, Michigan State University, East Lansing, Michigan 48824, USA*

^b*Research and Advanced Engineering, Ford Motor Company, Dearborn, MI 48121, USA*

^c*Department of Chemistry, Michigan State University, East Lansing, MI 48824, USA*

^d*Department of Biosystems and Agricultural Engineering, Michigan State University, East Lansing, MI 48824, USA*

Abstract

Maximizing fossil fuel displacement and limiting atmospheric carbon dioxide levels require a high efficiency of carbon incorporation in bioenergy systems. The availability of biomass carbon is a constraint globally, and strategies to increase the efficiency of bioenergy production and biogenic carbon use are needed. Previous studies have shown that “energy upgrading” of biomass by coupling with renewable electricity through electrocatalytic hydrogenation offers a potential pathway to near full petroleum fuel displacement in the U.S., even when annual U.S. biomass production is limited to 1.2 billion dry tonnes. Commercialization of such technology requires economic feasibility. A technoeconomic model of decentralized, depot-based pyrolysis with electrocatalytic hydrogenation and centralized upgrading (Py-ECH), producing liquid hydrocarbon fuel is presented and compared to a cellulosic ethanol pathway using consistent assumptions. Using a discounted cash flow approach, a minimum fuel selling price (MFSP) of \$3.62/gallon gasoline equivalent (GGE) or \$0.96/gasoline liter equivalent (GLE) is estimated for Py-ECH fuel derived from corn stover, considering n^{th} plant economics and a fixed internal rate of return of 10%. This is comparable to the MFSP for cellulosic ethanol from fermentation with the same feedstock (\$3.71/GGE or \$0.98/GLE) and is in the range of gasoline prices over the last 20 years of \$1/GGE (\$0.26/GLE) to \$4.44/GGE (\$1.17/GLE) in 2018\$. Optimization studies on depot sizing identified a trade-off between transportation and economies-of-scale costs, with an optimum size of 500 tpd. Sensitivity analyses showed that electricity cost, raw material costs, bio-oil yields, and cell efficiencies are the key parameters that affect the Py-ECH MFSP. With system improvements, a pathway to less than \$3/GGE or \$0.79/GLE is articulated for liquid hydrocarbon fuel from corn stover using Py-ECH.

1. Introduction

The U.S. Department of Energy's "2016 Billion-Ton Report" projected the total harvestable biomass available in the U.S. to be 1.3 billion dry tons by the year 2030 for biomass obtained at a cost of less than \$60/dry ton. While this is a large quantity, the carbon and energy content of this biomass is insufficient to meet the energy demands of the U.S. transportation sector. It is important to develop bioenergy systems that utilize renewable energy and carbon efficiently. Py-ECH has an advantage over cellulosic ethanol in terms of carbon efficiency, as one-third of the holocellulosic carbon is lost as carbon dioxide during fermentation.¹ Moreover, combusting lignin for internal heat and power also diverts carbon away from incorporation into higher-value liquid fuels.

Nearly all liquid biofuel strategies require biomass deconstruction as an early step in processing. The literature on deconstruction is immense and growing, as new techniques involving acids, bases, solvents, enzymes, heat, and combinations thereof continue to emerge. Of the many existing deconstruction techniques, biomass fast pyrolysis is well-studied and can be achieved with low capital cost and high yield because of short residence times. Further, it converts a portion of the biomass lignin along with the holocellulose into the primary product, bio-oil.¹⁻³ Regional biomass processing depots to produce bio-oil are capable of lowering overall hauling costs because bulk density is increased,⁴ however the reactivity of bio-oil limits its ability to be transported. Functional groups such as carbonyls, carboxylates, and alcohols react to form polymers which increase viscosity and form sludges. Further, bio-oil from pyrolysis is corrosive to metals as it contains weak acids and has high total acid number (TAN).

Bio-oil is unsuitable for transport and storage and needs to be stabilized immediately after pyrolysis. Thermal hydrogenation and hydrodeoxygenation have been used for hydrogenating and stabilizing bio-oil,^{3, 5-16} however, these techniques operate under high temperature and pressure and are not suited for widespread deployment in small-scale plants (depots).⁴ A milder alternative is electrocatalytic hydrogenation (ECH), which involves the electrolysis of water to produce *in-situ* hydrogen ions on the anode that electrocatalytically react with bio-oil on the cathode. This technique has been shown to successfully hydrogenate and deoxygenate the variety of compounds found in raw biomass-derived bio-oil as well as lignin-derived bio-oil.¹⁷⁻²³ ECH is a promising strategy because it operates at mild conditions, avoids storage or use of hydrogen gas, and also reduces hydrogen consumption at the centralized refinery where hydroprocessing can be safely

utilized to create finished fuels.^{17, 19} Sequential fast pyrolysis and electrocatalysis (Py-ECH) co-deployed in a biomass upgrading depot, followed by petroleum-style hydroprocessing in central refineries, potentially offers a carbon and energy efficient strategy for making liquid hydrocarbon biofuels.¹

While such a decentralized biorefinery system shows promise in terms of carbon and energy efficiency, its economics must be investigated. Technoeconomic analyses have been completed for centralized pyrolysis followed by hydroprocessing. Wright²⁴ et al. estimated a minimum fuel selling price (MFSP) of \$2.41/GGE (\$0.64/GLE) when the merchant H₂ is purchased at \$1.47/kg H₂ for hydroprocessing. (All costs herein are determined or converted to 2018\$.) However, when a portion of the bio-oil is steam reformed to make the H₂ gas required for upgrading the remaining bio-oil, the MFSP of the fuel increased to \$3.55/GGE (\$0.94/GLE). Brown et al.²⁵ estimated an MFSP of \$2.64/GGE (\$0.70/GLE) for a pyrolysis and hydroprocessing facility that processed 2,000 tonnes/day (tpd) of corn stover. Jones et al.²⁶ estimated the MFSP of a hydrocarbon fuel derived from pyrolysis and hydrotreating of hybrid poplar to be \$2.34/GGE (\$0.2/GLE). Dutta et al.²⁷ determined the MFSP of hydrocarbon fuel produced from the pyrolysis and vapor upgrading of lignocellulosic biomass to be in the range of \$3.41/GGE (\$0.9/GLE) to \$3.56/GGE (\$0.95/GLE), depending on whether the upgrading is done in-situ or ex-situ. Carrasco et al.²⁸ estimated the economics for pyrolysis and hydrotreating of forest residues to make liquid fuels and found an MFSP of \$6.64/GGE (\$1.75/GLE). These MFSPs fall in the range of \$2.17-\$7.24/GGE (\$0.54-\$1.8/GLE) reported by Sorunmu et al.²⁹ in their review of technoeconomic analyses for the pyrolysis and upgrading of lignocellulosic biomass. None of these systems, however, considered decentralized upgrading or the use of ECH.

Orella et al.³⁰ investigated the technoeconomics of the ECH process alone and developed a model to estimate the MFSP of reducing guaiacol, a pyrolysis bio-oil representative compound, to phenol. It was reported that with enhanced current density, decreased selectivity for hydrogen evolution and increased faradaic efficiencies for the desired product, the selling price for phenol can drop from \$28.67/kg to \$0.42/kg.

In the present work, a technoeconomic analysis has been performed for the full-scale combined Py-ECH process that upgrades biomass (corn stover) to a stable fuel intermediate in decentralized depots, which is then delivered to a centralized refinery that uses traditional hydroprocessing to produce a liquid hydrocarbon fuel. The produced liquid hydrocarbon fuel

mixture is assumed to have properties of iso-octane, representative of gasoline. This liquid hydrocarbon fuel is the major component of the refinery's finished fuel output. Sensitivity analyses were conducted to identify key parameters that influence the MFSP, with the objective of guiding researchers towards economically relevant process improvements. Unless specified otherwise, all costs are in 2018\$.

2. Materials and Methods

2.1. Process Description

The process under investigation combines fast pyrolysis of corn stover and subsequent electrocatalytic hydrogenation (Py-ECH) in depots with hydroprocessing in a central refinery to produce liquid fuels from biomass (Figure 1) as described in detail elsewhere.³¹ In brief, the Py-ECH system involves hauling biomass from the cultivation fields to regional depots where it is ground and dried prior to deconstruction in a fast pyrolysis reactor at 500°C and atmospheric pressure. The assumed mass percentages of the pyrolysis products are 70%, 15%, and 15% for liquid bio-oil, biochar, and non-condensable gases, respectively. The resultant bio-oil is then electrocatalytically reduced in an ECH unit at 80°C and atmospheric pressure. Ruthenium metal serves as the electrocatalyst. ECH-stabilized bio-oil is then transported to a central hydroprocessing facility where it is further upgraded to liquid hydrocarbon fuel using hydrogen at 400°C and 200 bar pressure in the presence of Co-Mo catalyst.³² The hydrogen is assumed to be renewably generated by electrolysis of water at the central refinery.

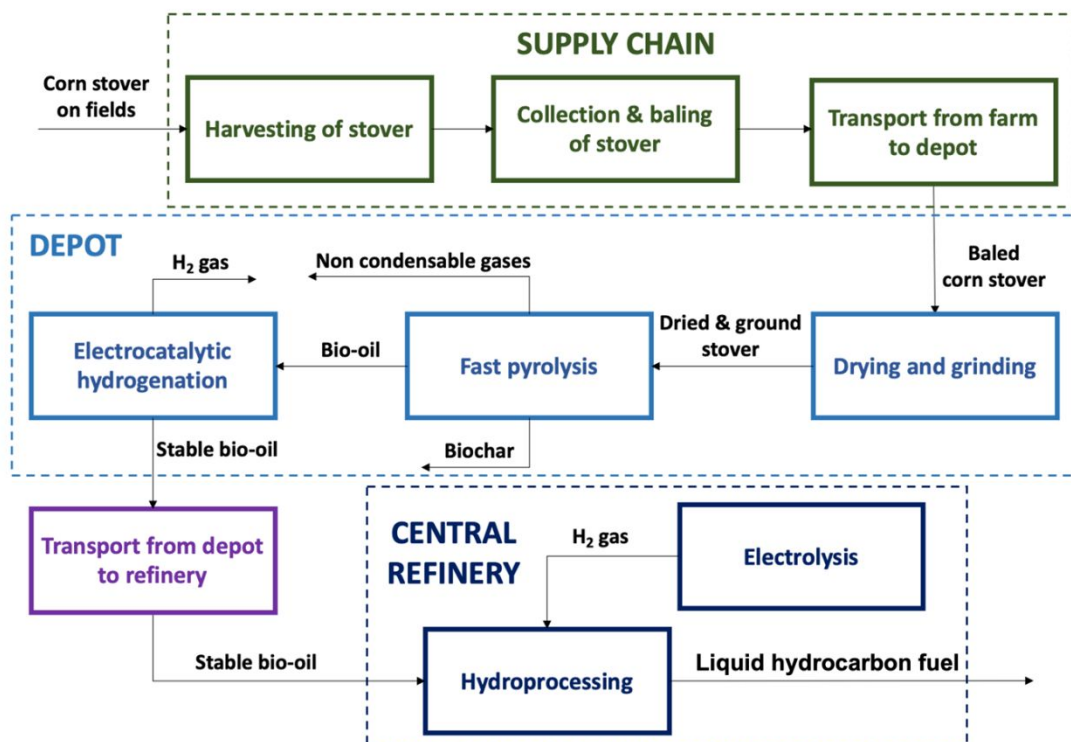


Figure 1: Py-ECH process flow diagram with pyrolysis and electrocatalytic hydrogenation in decentralized depots and hydroprocessing in centralized refineries.

Economics of cellulosic ethanol produced via fermentation of corn stover feedstock were evaluated using the analysis by Humbird et al.³³ at the National Renewable Energy Laboratory (NREL). The analysis was used as a framework for the Py-ECH analysis, using the same assumptions where possible and appropriate, including a 2,000 tonne/day biomass processing scale as the combined input to the system of Py-ECH depots. Multiple depots, equally sized, supply a single centralized refinery to make the finished hydrocarbon fuel component. Depot sizes in previous literature have varied, for example Eranki et al. reported values of 100 tpd⁴ and Lamers et al. assumed a maximum of 215 tpd.³⁴ The depot size in the present analysis was fixed after an optimization study that minimized the total system transportation cost, from fields to depots to central refinery. The assumed composition and moisture content of the delivered corn stover at the depot gate were the same as the Humbird et al. report.³³ Material and energy balances required for the Py-ECH and cellulosic ethanol economics were extracted from our previous work³¹ and the NREL study, respectively.

2.2. Economic Model

The economic modeling and assumptions for the Py-ECH system were consistent with that for an n^{th} plant in the Humbird et al. report for ethanol production via fermentation of cellulose.³³ The minimum fuel selling price (MFSP) of the fuel produced was determined using a discounted cash flow analysis (DCFA) with a fixed internal rate of return. This was performed by iterating the MFSP until the net present value of all cash flows for the entire plant life equaled zero. It must be noted that the DCFA was performed twice, first at the depot, and then at the central refinery. For the depot, the raw material was the corn stover biomass and the finished product was the ECH-stabilized bio-oil. For the central refinery, the raw material was this ECH-stabilized bio-oil and the product was isooctane, the final hydrocarbon fuel component.

Table 1: Assumptions in the technoeconomic model.

Parameter	Value
Plant life	30 years
Plant location	Midwest USA
Cost basis year	2018
Internal rate of return	10%
Depreciation method	200% double declining balance
Federal tax rate	35%
Working capital	5% of fixed capital investment
Salvage value	0 \$
Construction period	1 year
Startup period	3 months
Revenues during startup	50%
Variable costs during startup	75%
Fixed costs during startup	100%
Loan terms	8% APR; 10 years
Financing	40% equity

Economic assumptions for the technoeconomic modeling are summarized in Table 1. The total capital investment included fixed capital investment (FCI), land, and working capital (assumed 5% of FCI). The FCI, in turn, included both direct and indirect costs and were functions of the total installed equipment costs. Installed equipment costs were determined by applying an installation multiplier to the estimated equipment cost. Details behind these equipment costs are described in the Supplementary Information and a data inventory is given in Table S5. Operating costs were determined by summing the fixed costs (e.g., employee salaries, insurance, and maintenance costs) and variable costs (e.g., raw materials and utilities). While the fixed operating

costs were percentages of the total capital investment, the variable operating costs were either estimated from literature data or calculated. For instance, the raw material cost for the Py-ECH system was estimated from a supply chain analysis, described in the next section.

2.2.1. By-products

In addition to the ECH bio-oil, the Py-ECH system generates two by-products at the depot: biochar and H₂ from the ECH unit. While the biochar is not utilized in the process, some of the ECH H₂ is utilized, in combination with the non-condensable gases from the pyrolyzer, to meet the heat requirements at the depot. Excess H₂ and biochar may be sold for additional revenue to bring down the cost of the final Py-ECH fuel. This is similar to the approach adopted in the NREL cellulosic ethanol study in which revenue from selling excess electricity was incorporated to determine the final MFSP of the fuel. The H₂ price was fixed at \$2/kg, which is the U.S. Department of Energy 2020 total levelized cost target for generation from electrolysis.³⁵ This falls within the range for the cost of H₂ generated from steam reforming, from \$1.25/kg for large systems to \$3.50/kg for smaller systems.³⁶ There is a large range of estimated selling prices for biochar in the literature. Campbell et al. reviewed different biochar production scenarios and estimated selling prices from \$80/tonne to about \$13,000/tonne in 2013\$.³⁷ The selling price of biochar depends heavily on its quality as determined by its carbon and ash contents, the biomass source, and whether it is a wholesale or retail price, among other factors.³⁷ Table S2 in the supplementary information provides a range of biochar prices from the literature. Due to the high uncertainty in the value and quality of the biochar being generated, the baseline scenario of the present study assumes that biochar has no value and is not sold. A sensitivity analysis was conducted in which biochar was assigned a conservative value.

2.3. Supply Chain

The price of delivered corn stover for cellulosic fermentation to ethanol (CE) was taken from the Humbird et al. report and adjusted to 2018\$ using Chemical Engineering Plant Cost Indices.³⁸ Costs were originally estimated from the Department of Energy's Multi-Year Program Plan (MYPP) published in 2011. While the 2016 MYPP has since been published, we employed values from the 2011 report as the 2016 MYPP mostly explores blended feedstock with less focus on corn stover as the sole feedstock. The major components of the feedstock price are harvesting and collection, feedstock storage, preprocessing, transportation and handling, and the grower payment. To maintain consistency, the same assumptions were used for the Py-ECH system with a few

exceptions. The preprocessing costs involved drying and grinding operations, aimed at making the raw material fit for processing. These costs are included as separate unit operations at the depot and therefore excluded from the raw material cost for the Py-ECH system.

Another key difference between the two systems is logistics. While all corn stover is directly brought to a single cellulosic ethanol biorefinery in the CE system, transportation in the Py-ECH system occurs in two stages. Corn stover is first transported over short distances from fields to depots, and later the stable bio-oil is transported from the depots to the central refinery. To estimate the transportation cost of delivering raw corn stover to depots in the Py-ECH system, we conducted an optimization study to minimize the minimum fuel selling price (MFSP). Kim and Dale³⁹ reported an equation giving optimal depot size based on farm-to-depot transportation distance (see Table S3 and S4 of Supplementary Information). Kim and Dale assumed a solar-system-like model, where the refinery is located at the center, with all the depots located in rings around the refinery and with each depot having its own collection radius.

In the present analysis, a square geometry was assumed (as land is commonly parceled). Figure 2(a) shows one instance of an example configuration. The central refinery (red square) is located in the center, while the depots (black stars) are scattered around the refinery. The green squares represent the biomass collection area for the depot located at its center and are assumed to constitute 25% of the land area.⁴⁰ The white spaces denote the 75% not dedicated to crop cultivation. No depots were assumed to be located in the region adjacent to the refinery, denoted by the blue boundary, to avoid a situation where the biomass is closer to the refinery than the depot. The depot arrangement shown in Figure 2(a) is one of many arrangements, each with different average depot-to-refinery distance and consequently, different transportation costs. Therefore, optimization was performed for determining the optimal placement of the depots around the central refinery that resulted in the lowest total transportation cost. Figure 2 (b) shows how the depot-to-refinery distance, and the farm-to-depot distance varies with depot size for a 2,000 tonne/day central refinery. Further details are given in the supporting information.

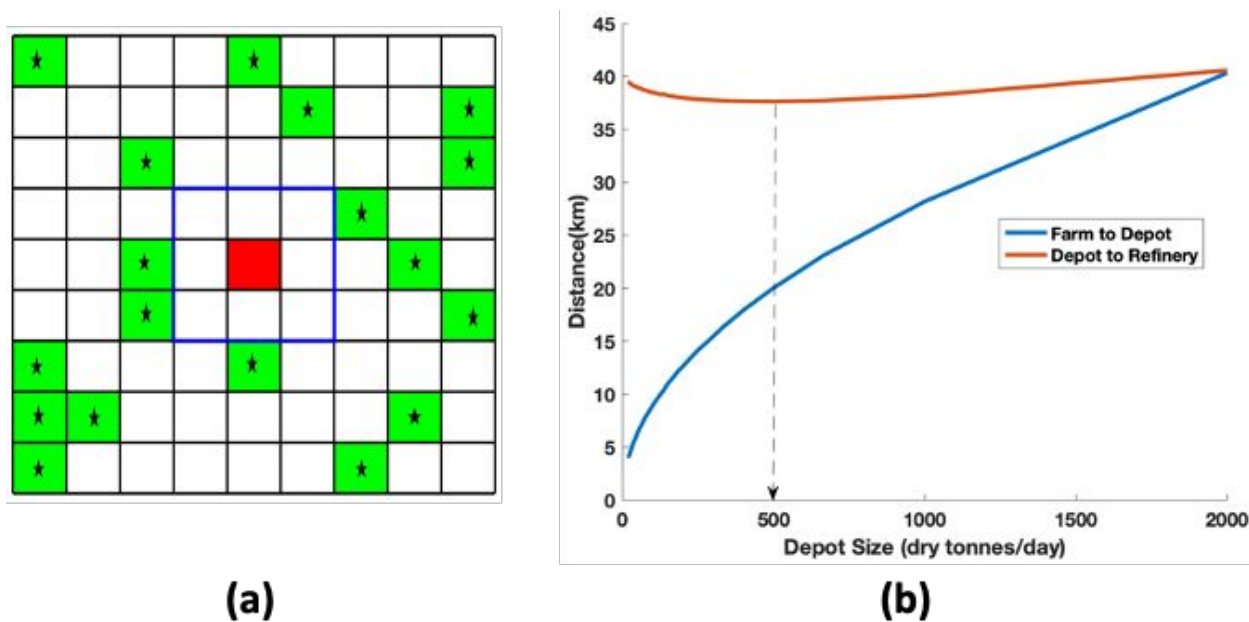


Figure 2: (a) Illustration of a random depot distribution (black stars) and their biomass collection areas (green squares) relative to central refinery (red square), for a central refinery with 18 depots. (b) farm-to-depot and depot-to-refinery distance versus depot size for a 2,000 tpd central refinery.

The farm-to-depot distance varies as the square root of the depot size as the land has been parceled into squares. The depot-to-refinery distance goes through a slight minimum at a depot size of 500 tpd but does not vary greatly for higher and lower sizes because the depots are fairly close together when the central refinery size is 2,000 tpd.

3. Results

3.1. Supply Chain Costs

Using the optimization strategy and the economic model outlined in the previous sections, the minimum fuel selling price (MFSP) was calculated for different depot and refinery sizes (Figure 3). For all refinery sizes (except for a 1,000 tpd central refinery), the MFSP passes through a minimum as depot sizes are increased. As depot size increases, the MFSP initially decreases reflecting economies-of-scale. For still larger depot sizes, longer field-to-depot distances overwhelm the economies-of-scale benefit. The minimum transportation cost occurs for depot sizes of 500-1,000 tpd, as highlighted in Figure 3 by dotted vertical lines. For a 1,000 tpd central refinery, a minimum was not observed as transportation distances are not large enough to overcome the improving economies-of-scale. It must be noted here that the sharp changes in slope

observed in the profile for some of the refinery sizes (e.g., for $C_R=10,000$ tpd) is due to the fact that the MFSP is not a continuous function of the depot size. Furthermore, the change in depot size is sometimes not large enough to effect an observable change in the MFSP. For the present analysis which assumes a refinery capacity of 2,000 tpd, the minimum was observed for a depot size of 500 tpd, i.e., 4 depots per refinery. This value is consistent with the minimum depot-to-refinery travel distance seen in Figure 2 (b).

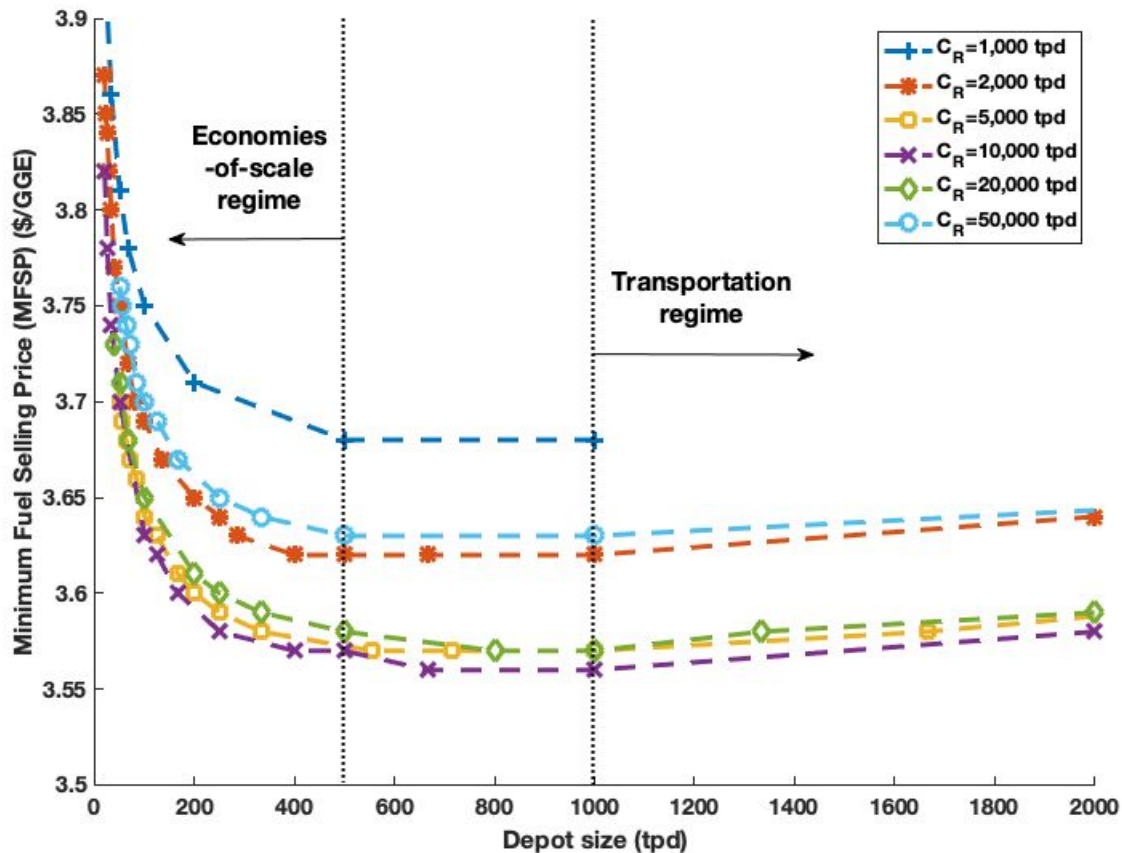


Figure 3: MFSP versus depot size for different central refinery processing capacities, C_R .

Next, the costs of transporting biomass from farm-to-depot and transporting the ECH bio-oil from depot-to-refinery were determined. Using the average farm-to-depot (24.7km) and depot-to-refinery distances (46.3 km) for the optimized depot arrangement with a trucking cost of \$1.82/mile (in 2018\$)⁴¹ gives a transport cost of \$2.97/tonne for biomass farm-to-depot delivery and a cost of \$7.71/tonne of ECH bio-oil delivered from a depot to a refinery. The total transportation cost for the Py-ECH system of \$7.82/ tonne of biomass is lower than the \$10/tonne of biomass assumed by Humbird et al. for the CE system, which highlights the advantage of

decentralization to reduce overall transport costs. The use of decentralized Py-ECH is the only difference between the two supply chains; all other costs related to biomass harvesting, collection and storage, and grower payments are the same. The total cost of delivered raw biomass is \$68.33/tonne of dry biomass for the CE system and \$61.30/tonne for the Py-ECH system. The relative contributions of different components of the two supply chains are shown in Figure 4 (a) and 4 (b) and the absolute values are reported in Table S4. The grower payment, which includes the cost of corn stover production and the growers' profit margin, dominate both systems. This is followed by the costs associated with harvesting, baling, and collecting stover. The major difference between the two systems is transportation: 15% of the supply chain costs in the CE system, but only 5% in the Py-ECH system. It must, however, be noted here that this transportation does not include the costs of transporting the ECH bio-oil from the depot to the refinery for the Py-ECH system.

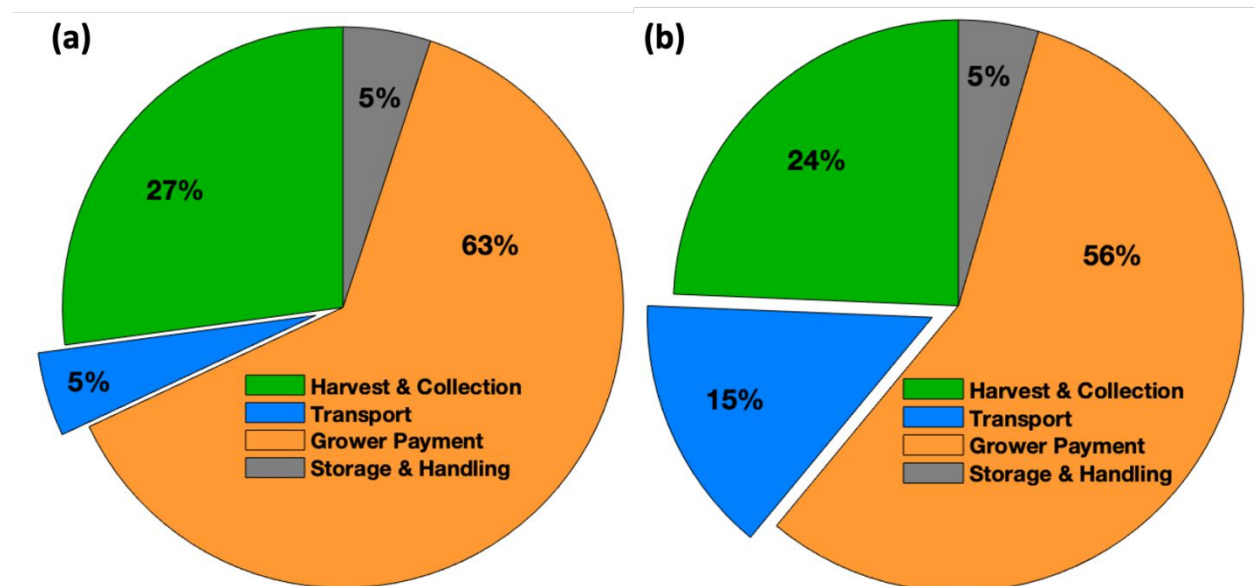


Figure 4: Raw material supply chain costs from farm to depot gate for Py-ECH (a) and from farm to refinery for CE system (b).

3.2. Depot Costs

Table 2 and Figure 5 show the capital and operating costs at a 500 tpd Py-ECH depot. The total capital investment for a single depot is \$29M, while the annual operating costs are about \$25M.

Capital costs at the depot are dominated by the ECH unit (67%) followed by the pyrolysis, combustion, and drying units. This reflects the high cost of the membrane electrode assembly stacks that are made of expensive noble metals (Pt anode and Ru cathode). Combustion, pyrolysis, and drying are the next highest costs, as high-temperature reaction vessels are used. The variable operating costs at the depot include the costs of raw materials, electricity, fresh water for ECH, and ECH stack replacement. Grid electricity (assumed at \$0.0656/kWh)³³ is about 63% of operating costs, reflecting the large electric energy requirement of ECH. Raw material costs (36%) are also significant because of the various supply chain costs already described. ECH stack replacement costs, assumed at 15% of the installed capital costs with a replacement schedule of 7 years are negligible (<1%), as seen in Figure 5(b).

Table 2: Depot Capital and Operating Costs (500 tpd Depot)

Unit	Total Capital Cost (2018\$)	
	Installed Cost	Percentage (%)
<i>Drying</i>	1,240,000	8.3
<i>Grinding</i>	167,000	1.1
<i>Pyrolysis</i>	1,300,000	8.8
<i>Condensation</i>	14,500	0.1
<i>ECH</i>	9,920,000	66.6
<i>Combustion</i>	1,490,000	10.0
<i>Storage</i>	758,000	5.1
Total Installed Capital Cost	14,900,000	100.0
Inside Battery Limits Capital Cost	12,600,000	
Direct Costs		
<i>Total Installed Capital Cost</i>	14,900,000	87.1
<i>Warehouse</i>	505,000	3.0
<i>Site Development</i>	1,140,000	6.6
<i>Additional Piping</i>	569,000	3.3
Total Direct Costs	17,100,000	100.0
Indirect Costs		
<i>Proratable Costs</i>	1,710,000	16.7
<i>Field Expenses</i>	1,710,000	16.7
<i>Home Office and Construction</i>	3,420,000	33.3
<i>Project Contingency</i>	1,710,000	16.7
<i>Other Costs</i>	1,710,000	16.6
Total Indirect Costs	10,300,000	100.0
Fixed Capital Investment (FCI)	27,400,000	94.5

Land	238,000	0.8
Working Capital	1,370,000	4.7
Total Capital Investment (TCI)	29,000,000	100.0
Total Operating Costs (2018\$/yr)		
Variable Operating Costs		
<i>Raw Material</i>	8,840,000	35.8
<i>Grid Electricity</i>	15,600,000	63.2
<i>Fresh Water</i>	19,700	0.1
<i>ECH Stack Replacement</i>	212,000	0.9
Total Variable Operating Costs	24,700,000	100.0
Fixed Operating Costs		
<i>Salaries</i>	145,000	17.1
<i>Labor</i>	130,000	15.4
<i>Maintenance</i>	379,000	44.8
<i>Property Insurance</i>	192,000	22.7
Total Fixed Operating Costs	846,000	100.0
Total Variable Operating Costs	24,700,000	96.7
Total Fixed Operating Costs	846,000	3.3
Total Operating Costs	25,500,000	100.0

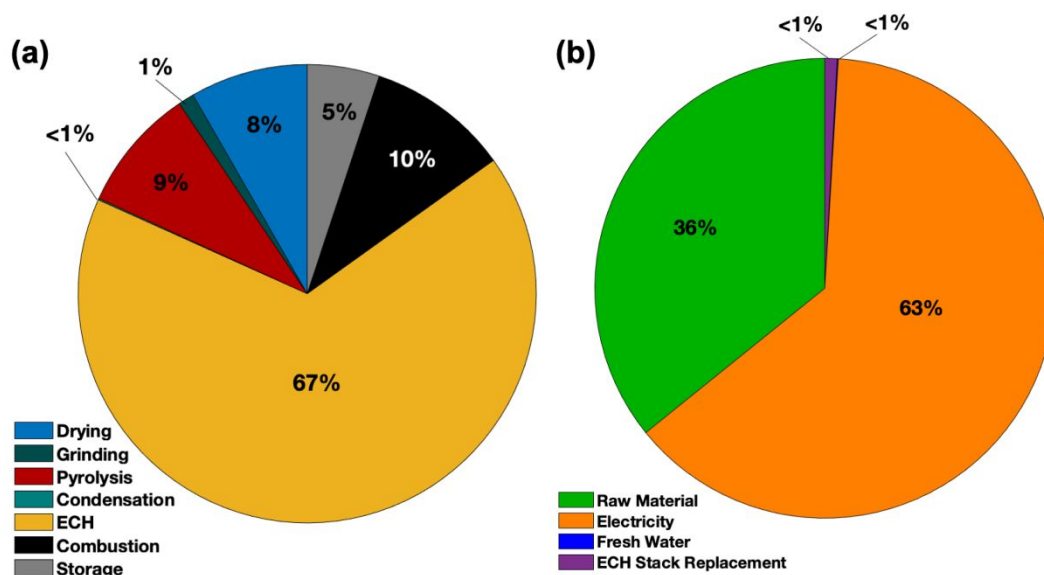


Figure 5: (a) Capital cost breakdown for a 500 tpd depot (b) Variable operating cost breakdown for a 500 tpd depot

3.3. Refinery Costs

Table 3 shows the estimated capital and operating costs at the refinery. The total capital investment for the central refinery is \$227M for processing the amount of bio-oil generated from pyrolyzing a total of 2,000 tpd of raw biomass from all the depots combined. The annual operating costs are around \$161M.

Table 3: Refinery Capital and Operating Costs (2000 tpd Refinery)

Unit	Total Capital Cost (2018\$)	
	Installed Cost	Percentage (%)
<i>Hydroprocessing</i>	47,900,000	42.0
<i>Electrolysis</i>	66,000,000	57.8
<i>Storage</i>	210,000	0.2
Total Installed Capital Cost	114,000,000	100.0
Inside Battery Limits Capital Cost	114,000,000	
Direct Costs		
<i>Total Installed Capital Cost</i>	114,000,000	85.1
<i>Warehouse</i>	4,560,000	3.4
<i>Site Development</i>	10,300,000	7.7
<i>Additional Piping</i>	5,130,000	3.8
Total Direct Costs	134,000,000	100.0
Indirect Costs		
<i>Proratable Costs</i>	13,400,000	16.7
<i>Field Expenses</i>	13,400,000	16.7
<i>Home Office and Construction</i>	26,800,000	33.3
<i>Project Contingency</i>	13,400,000	16.7
<i>Other Costs</i>	13,400,000	16.6
Total Indirect Costs	80,400,000	100.0
Fixed Capital Investment (FCI)	215,000,000	94.47
Land	183,000,000	0.80
Working Capital	10,700,000	4.72
Total Capital Investment (TCI)	227,000,000	100.00
Total Operating Costs (2018\$/yr)		
Variable Operating Costs		
<i>Raw Material</i>	100,000,000	65.1
<i>Grid Electricity</i>	42,700,000	27.6
<i>Natural Gas</i>	7,230,000	4.7
<i>Electrolyser Stack Replacement</i>	1,410,000	0.9
<i>Hydroprocessor Catalyst Replacement</i>	2,640,000	1.7
Total Variable Operating Costs	154,000,000	100.0

Fixed Operating Costs

Salaries	1,140,000	16.1
Labor Burden	1,020,000	14.4
Maintenance	3,420,000	48.3
Property Insurance	1,500,000	21.2
Total Fixed Operating Costs	7,080,000	100.0
Total Variable Operating Costs	154,000,000	95.6
Total Variable Operating Costs	154,000,000	4.4
Total Operating Costs	161,000,000	100.0

The refinery electrolyzer costs account for 58% of the total capital, while hydroprocessing comprises most of the remaining 42% as shown in Figure 6(a). The high costs for the electrolyzer are again attributed to the high cost of the membrane electrode assembly stacks in the electrolyzer.

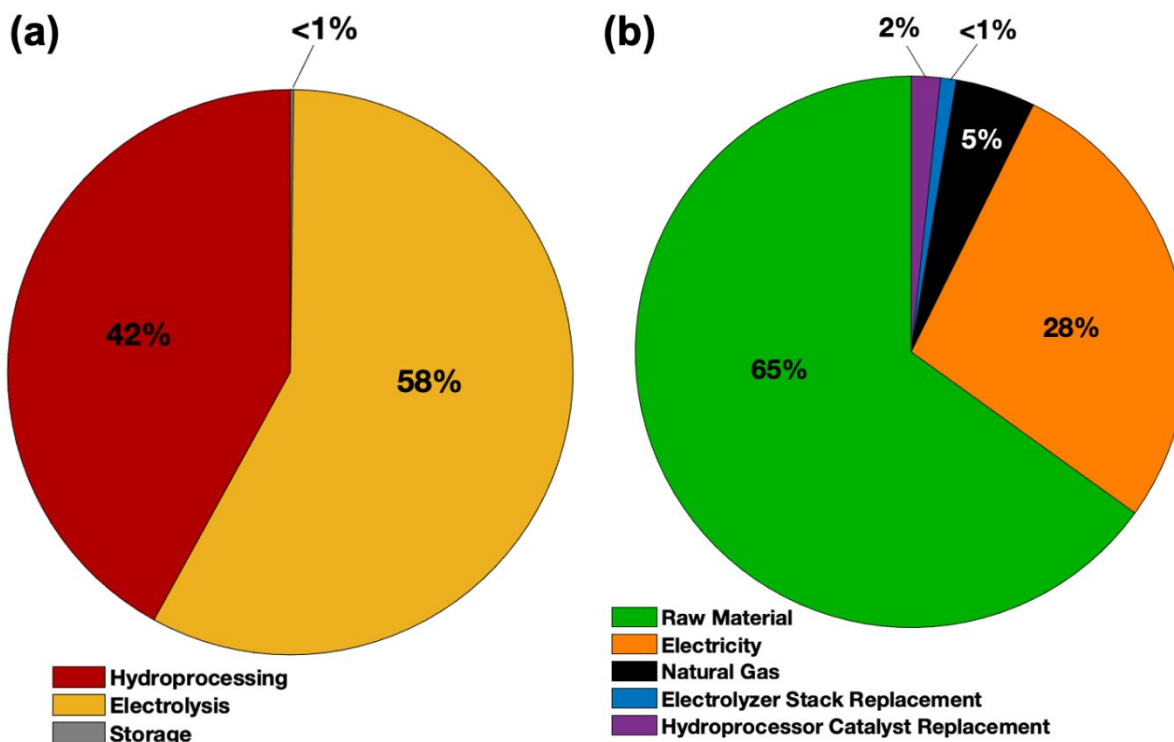


Figure 6: Refinery capital (a) and variable operating cost (b) breakdown.

The refinery variable operating costs in Figure 6(b) include raw material (stable bio-oil procured from the depots), electricity for the electrolyzer to produce H₂ gas, natural gas for process heating, electrolyser stack replacement, and hydroprocessing catalyst replacement costs. The chief

contributor to operating costs (65%) is the raw material purchased from the depots. This is essentially the MFSP (considering an internal rate of return of 10%) of the ECH bio-oil at the depot exit plus the cost of transporting the stable bio-oil from the depot to the refinery (3.4% of the raw material costs). Electricity accounts for 28% of the operating costs at the refinery, natural gas accounts for 5%, and other costs are negligible.

3.4. Minimum Fuel Selling Price

Technoeconomic analysis of the Py-ECH system, using a DCFA approach with an internal rate of return of 10%, yields an MFSP of **\$1.17/GGE (\$0.31/GLE)** for the stable bio-oil produced by the depot and an MFSP of **\$3.62/GGE (\$0.96/GLE)** for the fuel component produced by the refinery. For comparison, the MFSP for cellulosic ethanol was calculated to be \$2.47/gallon (\$3.71/GGE or \$0.98/GLE). Therefore, under the current assumptions, Py-ECH fuel is slightly cheaper than the cellulosic ethanol product on an energy basis. As a hydrocarbon product, the Py-ECH fuel has advantages over ethanol such as higher theoretical blending levels in gasoline or diesel fuel, compatibility with the conventional fuel distribution infrastructure and vehicles, and greater volumetric energy density. The extent to which the Py-ECH-HP hydrocarbons could be blended into gasoline or diesel will depend on its molecular size and structure, which determines its volatility and octane or cetane value.

3.5. Sensitivity Analyses

3.5.1. Effect of model parameters

Sensitivity analyses were performed to determine the key parameters affecting the MFSP of the Py-ECH fuel product. Electricity cost, raw material cost, bio-oil yield, internal rate of return (IRR), electrocatalytic cell efficiencies, catalyst price and thickness, costs associated with catalyst replacement, capital costs at depot and refinery, and the selling price of by-product hydrogen were investigated. The values of these parameters were changed by either 50% or 25%, and the results are shown as a tornado chart in Figure 7. A 25% change was only employed when a 50% change from the baseline value was impractical, e.g., a 50% increase in the assumed 70% bio-oil yield is not possible. Electricity and raw material costs are the most sensitive parameters in determining MFSP. This is intuitive since the Py-ECH system is a major consumer of electricity and raw materials are the other major cost contributor. Bio-oil yield, current and voltage efficiencies, the

assumed internal rate of return, and catalyst price and thickness are also important. An increase in bio-oil yield and the cell efficiencies leads to reduced losses in the system and an increase in the overall yield of the final fuel. The ECH catalyst price and thickness are also sensitive parameters. The catalyst replacement costs, whether in the ECH at the depot or the hydroprocessor at the central refinery, are not sensitive parameters because the replacement schedule of the ECH stack requires 15% of the installed capital cost of the stack every seven years. Similarly, the MFSP is relatively insensitive to the capital costs at the depot and refinery. Of the eight most sensitive parameters, five are directly linked to the ECH unit. Of the remaining three, two are related to the pyrolysis unit and one, the IRR, is an economic parameter that impacts all system costs. As both the pyrolysis and ECH units are at the depot, the sensitivity analysis points towards opportunities at the depot for further optimizing the economics of the Py-ECH-HP system. Attention could be focused on optimizing the ECH catalyst, process conditions, and efficiencies in comparison to equipment capital costs.

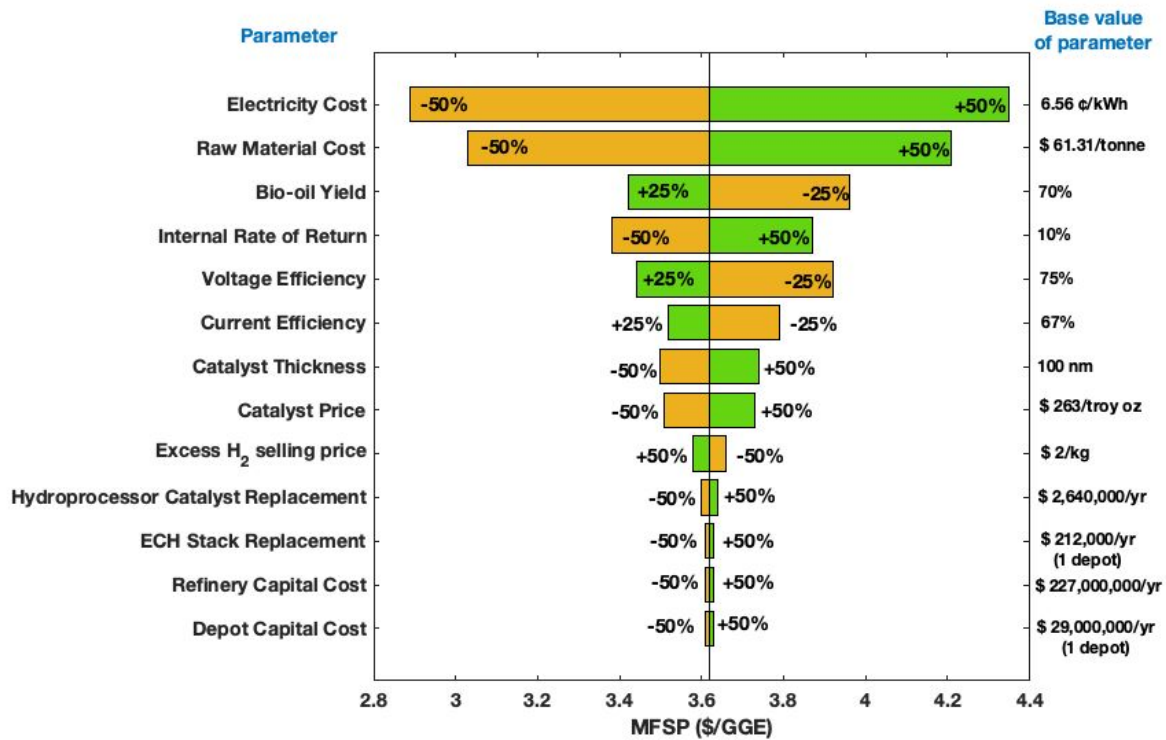


Figure 7: Tornado plot showing MFSP single parameter sensitivity analyses for the Py-ECH-HP system (Depot size of 500 tpd and refinery size of 2000 tpd)

3.5.2. Effect of Refinery Size

Consistent with the Humbird et al. cellulosic ethanol process analysis, the baseline refinery size was assumed to be 2,000 tpd. Additionally, variation of MFSP with refinery size for different depot sizes was investigated, as shown in Figure 8. Similar to the optimization of depot size in Figure 2, the MFSP goes through a minimum as refinery sizes are increased. For small refineries, poor economies-of-scale yield higher costs; for large refineries larger transportation costs dominate. These two forces lead to minimum MFSP at refinery sizes of 10,000-12,000 tpd. The sharp changes in the profiles are attributed to the same reasons as described for Figure 2.

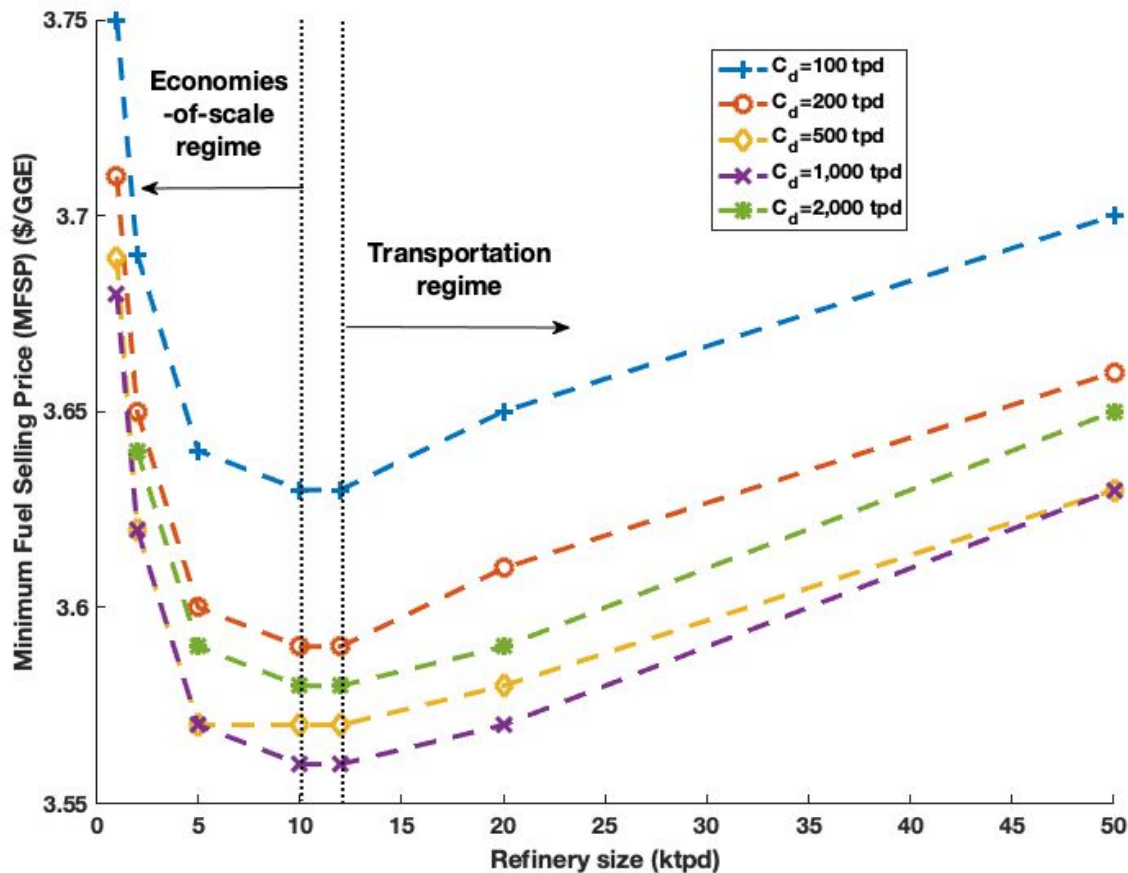


Figure 8: MFSP versus refinery size for different depot capacities, C_d .

As shown in Figure 8, an MFSP of \$3.56/GGE (\$0.94/GLE) is achieved for a refinery size of 10,000 tpd employing 10 depots, each having a capacity of 1,000 tpd. This cost reduction with higher central refinery scale is significant for the Py-ECH system, irrespective of the comparison to the CE system.

4. Discussion

While an MFSP of \$3.62/GGE (\$0.95/GLE) for Py-ECH fuel is slightly lower than the \$3.71/GGE (\$0.98/GLE) for ethanol in the CE system, a long-term goal is to be competitive with fossil gasoline and diesel prices. In this regard, the sensitivity analysis (Figure 7) points to opportunities for cost improvement: electricity cost, bio-oil yield, raw material cost, cell efficiencies, catalyst price and thickness, and the internal rate of return. However, it is difficult to improve upon the values assumed in the present model for some of these parameters. For example, the pyrolysis bio-oil yield has been assumed at 70%, which is among the highest values in the literature. Raw material costs have already been fairly well optimized by reducing the transport costs via the decentralized approach in the present model, leaving little opportunity for improvement, though waste biomass may be available at much lower price.

Utilizing low-cost electricity would be of great benefit to the Py-ECH system. While electricity has been assumed to cost \$0.066/kWh in the model, future costs as low as \$0.030/kWh are projected for wind and solar photovoltaics with advances in materials and manufacturing improvements.⁴² The U.S. Department of Energy's EIA⁴³ reports the levelized cost of renewable electricity, without tax credits, ranging from \$0.039/kWh (hydroelectric) to \$0.157/kWh (solar thermal). The effect on MFSP of using these different electricity sources is explored in Figure S2. The Wind Energy Technologies Office at the U.S. Department of Energy estimates a price of \$0.010-0.020/kWh for electricity produced from wind sources, after applying a production tax credit. Reducing the electricity price to \$0.030/kWh results in a \$0.65/GGE (\$0.17/GLE) drop in the MFSP for Py-ECH fuel.

A current efficiency of 67% was assumed in the current model, but An et al. have reported current efficiencies of 70% for hydrogenation of soybean oil in a solid polymer electrolyte reactor when hydrogen is generated from electrolysis of water.⁴⁴ Pintauro et al. report current efficiencies as high as 97% when hydrogen gas was used for electrochemical hydrogenation of soybean oil.⁴⁵ Therefore an improvement in current efficiency from 67% to 95% may be achievable and this would lead to a further \$0.15/GGE (\$0.04/GLE) reduction in MFSP.

The catalyst (Ru) price, assumed at the 2019 price of \$263/troy oz, has ranged from \$40-270/troy oz over the last 10 years with an average of approximately \$121/troy oz.⁴⁶ Prices rose to \$180/troy oz in 2011, dipped to around \$40/troy oz in 2016, then climbed to \$270/troy oz in 2019. Using the 10-year average price of \$121/troy oz in our calculations results in a further \$0.08/GGE decrease in the MFSP.

Potential future improvements in voltage efficiencies and reductions in thickness of the ECH catalyst layer are difficult to estimate due to lack of information and were not considered further. As explored in the previous section, increasing the refinery size from the assumed 2,000 tpd to the optimum 10,000 tpd further lowered the MFSP by \$0.06/GGE. Finally, reducing the ECH stack replacement cost (changing replacement from 15% of installed capital costs every 7 years to 12% of installed capital costs every 10 years) yielded a very low cost reduction.⁴⁷ The final MFSP after stacking all the improvements is \$ 2.67/GGE (\$0.71/GLE) and is shown in the green bar at the extreme right in Figure 9.

A further reduction in MFSP may be achieved by selling the by-product biochar generated at the depot. This was not considered in the base case analysis as information is lacking about the produced biochar quality and uncertainty about the price that could be obtained. Therefore, it is handled as an alternative scenario, represented by the grey bar on the right which assumes biochar can be sold at \$78.26/tonne (the most conservative literature value found),³⁷ further reducing the final MFSP of the Py-ECH fuel to \$2.57/GGE (\$0.68/GLE).

The reductions in MFSP gained by stacking these improvements are shown in Figure 9. Figure 9 also highlights the benefit of optimizing the transportation costs in the decentralized Py-ECH system, as shown by the yellow bar on the extreme left. The unoptimized transportation cost leads to a feedstock cost of \$68.33/dry tonne (as assumed in the CE system by Humbird et al.), which results in an MFSP of \$3.76/GGE (\$0.99/GLE). Optimization of transportation costs reduces the MFSP by \$0.14/GGE (\$0.037/GLE).

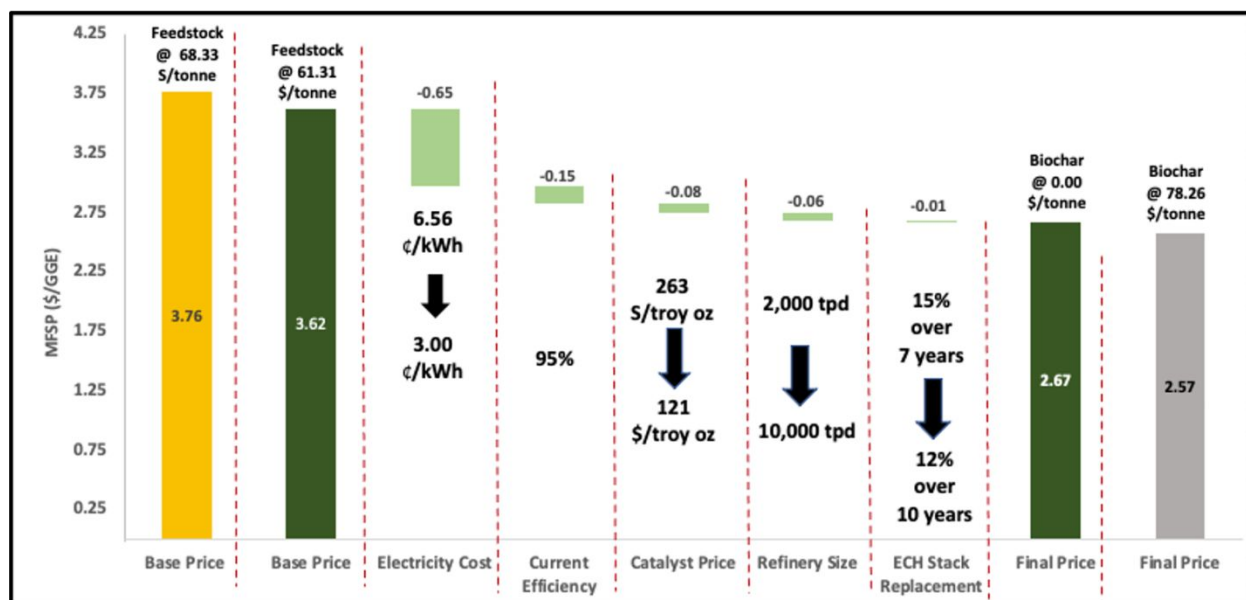


Figure 9: Waterfall chart showing potential reduction in MFSP assuming combinations of improvements in model parameters. The light green bars show MFSP reductions from “stacking” of system improvements. The dark green bars show initial and final MFSP (after all improvements). The yellow bar at the extreme left shows the scenario when the biomass supply chain is not optimized. The grey bar at the extreme right shows the scenario when biochar is sold as a by-product.

Our techno-economic analysis for the Py-ECH system (where four 500 tonne/day depots process corn stover and supply ECH-stabilized bio-oil to a central refinery for further hydroprocessing) yields a projected MFSP of \$3.62/GGE (\$0.96/GLE) for the final hydrocarbon fuel component. This MFSP is slightly lower than ethanol from cellulosic ethanol refineries (\$3.71/GGE or \$0.98/GLE) using consistent assumptions. Pathways for further reductions in MFSP were determined by varying key parameters in a sensitivity analysis. Sensitive parameters were electricity cost, raw material costs, pyrolysis bio-oil yield, ECH current efficiencies, and the price and thickness of the ECH catalyst. Stacking feasible improvements can reduce the MFSP to \$2.67/GGE (\$0.71/GLE), which is further reduced to \$2.57/GGE (\$0.68/GLE) if the by-product biochar is sold at approximately \$80/tonne.

We have shown previously that compared to microbial bioconversion, the Py-ECH process enables significantly higher yields of renewable hydrocarbon fuels and offers a large-scale mechanism for chemical storage of renewable but intermittently generated electrical energy as transportation fuel.¹ Here we estimate MFSPs of Py-ECH renewable hydrocarbon fuels in the range of \$2.7-3.7/GGE (\$0.71-0.98/GLE). This range is easily competitive with the MFSPs of

hydrocarbon fuels found in literature, generated from centralized upgrading of pyrolysis bio-oils via hydrogen addition. Sorunmu et al.,²⁹ in their 2019 review, estimates this range as \$2.17-7.24/GGE (\$0.54-0.80/GLE). Decentralized pyrolysis and partial upgrading of biomass results in MFSPs towards the lower end of the range. One of the lowest MFSPs, \$2.34/GGE (\$0.62/GLE), assumes a feedstock cost of \$58/dry ton with 50% moisture, which amounts to \$33/tonne of biomass, compared to \$61/tonne that is assumed in this analysis. In fact, the MFSP estimated here would be competitive to fossil gasoline and diesel prices at the higher end of their historic range of approximately \$1-4/GGE (\$0.26-1.06/GLE). If alternatives are successful, it would be expected that fossil gasoline and diesel prices would be driven to the lower end of their historical range. With the system described in the present study, Py-ECH renewable hydrocarbon fuels produced using renewable electricity have a least 90% lower lifecycle CO₂ emissions than gasoline, as documented in a life cycle analysis that is currently under review. In this regard, a carbon abatement subsidy or CO₂ production cost²⁹ would reduce the gap between decentralized biofuel and fossil gasoline/diesel prices. These incentives for producing fuels with lesser GHG emissions may be combined with other subsidies, including those for certain feedstocks, output-based incentives and capital grants to further lower biofuel MFSPs.⁴⁸ Future studies that incorporate carbon policies and incentives would be complementary to the present technoeconomic analysis.

Acknowledgements

This work was funded in part by the Ford Motor Company and the National Science Foundation under award number 2055068. Dr. Saffron's contribution was supported in part by the USDA National Institute of Food and Agriculture, Hatch project 1018335, and Michigan State University AgBioResearch.

References

1. A. V. Bridgwater, *Fast Pyrolysis of Biomass: A Handbook Volume 2*, CPL Press, 2008.
2. A. Bridgwater, D. Meier and D. Radlein, *Organic Geochemistry*, 1999, **30**, 1479-1493.
3. A. V. Bridgwater, *Biomass and bioenergy*, 2012, **38**, 68-94.
4. P. L. Eranki, B. D. Bals and B. E. Dale, *Biofuels, Bioproducts and Biorefining*, 2011, **5**, 621-630.
5. E. Furimsky, *Applied Catalysis A: General*, 2000, **199**, 147-190.
6. V. N. Bui, D. Laurenti, P. Afanasiev and C. Geantet, *Applied Catalysis B: Environmental*, 2011, **101**, 239-245.
7. R. C. Baliban, J. A. Elia and C. A. Floudas, *Energy & Environmental Science*, 2013, **6**, 267-287.

8. R. Rinaldi and F. Schüth, *Energy & Environmental Science*, 2009, **2**, 610-626.
9. J. C. Serrano-Ruiz and J. A. Dumesic, *Energy & Environmental Science*, 2011, **4**, 83-99.
10. C. Zhao, Y. Kou, A. A. Lemonidou, X. Li and J. A. Lercher, *Angewandte Chemie*, 2009, **121**, 4047-4050.
11. T. Choudhary and C. Phillips, *Applied Catalysis A: General*, 2011, **397**, 1-12.
12. D. C. Elliott and T. R. Hart, *Energy & Fuels*, 2008, **23**, 631-637.
13. J. Wildschut, F. H. Mahfud, R. H. Venderbosch and H. J. Heeres, *Industrial & Engineering Chemistry Research*, 2009, **48**, 10324-10334.
14. D. A. Ruddy, J. A. Schaidle, J. R. Ferrell III, J. Wang, L. Moens and J. E. Hensley, *Green Chemistry*, 2014, **16**, 454-490.
15. M. Saidi, F. Samimi, D. Karimipourfard, T. Nimmanwudipong, B. C. Gates and M. R. Rahimpour, *Energy & Environmental Science*, 2014, **7**, 103-129.
16. S. Czernik and A. Bridgwater, *Energy & fuels*, 2004, **18**, 590-598.
17. Z. Li, M. Garedew, C. H. Lam, J. E. Jackson, D. J. Miller and C. M. Saffron, *Green Chemistry*, 2012, **14**, 2540-2549.
18. Z. Li, S. Kelkar, L. Raycraft, M. Garedew, J. E. Jackson, D. J. Miller and C. M. Saffron, *Green Chemistry*, 2014, **16**, 844-852.
19. C. H. Lam, C. B. Lowe, Z. Li, K. N. Longe, J. T. Rayburn, M. A. Caldwell, C. E. Houdek, J. B. Maguire, C. M. Saffron, D. J. Miller and J. E. Jackson, *Green Chem.*, 2015, **17**, 601-609.
20. M. Garedew, D. Young-Farhat, S. Bhatia, P. Hao, J. E. Jackson and C. M. Saffron, *Sustainable energy & fuels*, 2020, DOI: 10.1039/C9SE00912D.
21. M. Garedew, D. Young-Farhat, J. E. Jackson and C. M. Saffron, *ACS Sustainable Chemistry & Engineering*, 2019, **7**, 8375-8386.
22. Y. Zhou, G. E. Klinger, E. L. Hegg, C. M. Saffron and J. E. Jackson, *Journal of the American Chemical Society*, 2020, DOI: 10.1021/jacs.0c00199.
23. M. Garedew, C. H. Lam, L. Petitjean, S. Huang, B. Song, F. Lin, J. E. Jackson, C. M. Saffron and P. Anastas, *Green Chemistry*, 2021.
24. M. M. Wright, D. E. Dugaard, J. A. Satrio and R. C. Brown, *Fuel*, 2010, **89**, S2-S10.
25. T. R. Brown, R. Thilakaratne, R. C. Brown and G. Hu, *Fuel*, 2013, **106**, 463-469.
26. S. B. Jones, C. Valkenburt, C. W. Walton, D. C. Elliott, J. E. Holladay, D. J. Stevens, C. Kinchin and S. Czernik, *Production of gasoline and diesel from biomass via fast pyrolysis, hydrotreating and hydrocracking: a design case*, Pacific Northwest National Lab.(PNNL), Richland, WA (United States), 2009.
27. A. Dutta, A. Sahir, E. Tan, D. Humbird, L. J. Snowden-Swan, P. Meyer, J. Ross, D. Sexton, R. Yap and J. Lukas, *Process Design and Economics for the Conversion of Lignocellulosic Biomass to Hydrocarbon Fuels*, Report NREL/TP-5100-62455, PNNL-23823, NREL, PNNL, 2015.
28. J. L. Carrasco, S. Gunukula, A. A. Boateng, C. A. Mullen, W. J. DeSisto and M. C. Wheeler, *Fuel*, 2017, **193**, 477-484.
29. Y. Sorunmu, P. Billen and S. Spatari, *GCB Bioenergy*, 2020, **12**, 4-18.
30. M. J. Orella, S. M. Brown, M. E. Leonard, Y. Román-Leshkov and F. R. Brushett, *Energy Technology*, 2020, DOI: 10.1002/ente.201900994.

31. C. H. Lam, S. Das, N. C. Erickson, C. D. Hyzer, M. Garedew, J. E. Anderson, T. J. Wallington, M. A. Tamor, J. E. Jackson and C. M. Saffron, *Sustainable Energy & Fuels*, 2017, **1**, 258-266.
32. A. S. A. Dutta, E. Tan, D. Humbird, L.J. Snowden-Swan, P. Meyer, J. Ross, D. Sexton, R. Yap, J. Lukas, *Process Design and Economics for the Conversion of Lignocellulosic Biomass to Hydrocarbon Fuels*, Report NREL/TP-5100-62455, PNNL-23823, NREL, PNNL, 2015.
33. D. Humbird, R. Davis, L. Tao, C. Kinchin, D. Hsu, A. Aden, P. Schoen, J. Lukas, B. Olthof and M. Worley, *Process design and economics for biochemical conversion of lignocellulosic biomass to ethanol: dilute-acid pretreatment and enzymatic hydrolysis of corn stover*, Report NREL/TP-5100-47764, National Renewable Energy Laboratory (NREL), Golden, CO., 2011.
34. P. Lamers, M. S. Roni, J. S. Tumuluru, J. J. Jacobson, K. G. Cafferty, J. K. Hansen, K. Kenney, F. Teymouri and B. Bals, *Bioresource Technology*, 2015, **194**, 205-213.
35. DOE Technical Targets for Hydrogen Production from Electrolysis, <https://www.energy.gov/eere/fuelcells/doe-technical-targets-hydrogen-production-electrolysis#:~:text=The%202020%20target%20is%20based,year%20is%20set%20to%202025.>, (2020).
36. A. Ouammi, C. Bersani, R. Sacile and H. Dagdougui, *Hydrogen Infrastructure for Energy Applications: Production, Storage, Distribution and Safety*, Elsevier Academic Press, 2018.
37. R. M. Campbell, N. M. Anderson, D. E. Daugaard and H. T. Naughton, *Applied Energy*, 2018, **230**, 330-343.
38. M. Peters and K. Timmerhaus, *Plant design and economics for chemical engineers*, McGraw Hill, New York, 1980.
39. S. Kim and B. E. Dale, *Biomass and Bioenergy*, 2015, **74**, 135-147.
40. S. Sokhansanj, S. Mani, A. Turhollow, A. Kumar, D. Bransby, L. Lynd and M. Laser, *Biofuels, Bioproducts and Biorefining*, 2009, **3**, 124-141.
41. A. Hooper and D. Murray, *An Analysis of the Operational Costs of Trucking: 2018 Update*, 2018.
42. M. J. Orella, Y. Román-Leshkov and F. R. Brushett, *Current Opinion in Chemical Engineering*, 2018, **20**, 159-167.
43. *Levelized Cost and Levelized Avoided Cost of New Generation Resources in the Annual Energy Outlook 2019*, United States Energy Information Administration, 2019.
44. W. An, J. Hong and P. Pintauro, *Journal of applied electrochemistry*, 1998, **28**, 947-954.
45. P. N. Pintauro, M. P. Gil, K. Warner, G. List and W. Neff, *Industrial & Engineering Chemistry Research*, 2005, **44**, 6188-6195.
46. Ruthenium Price Chart, <http://www.platinum.matthey.com/prices/price-charts#>.
47. D. Peterson, J. Vickers and D. DeSantis, *Hydrogen Production Cost From PEM Electrolysis - 2019, 2020*.
48. Z. J. Wang, M. D. Staples, W. E. Tyner, X. Zhao, R. Malina, H. Olcay, F. Allroggen and S. R. H. Barrett, *Frontiers in Energy Research*, 2021, **9**.